

Entire-Domain Basis MOM Analysis of Coupled Microstrip Transmission Lines

Jonathan S. Bagby, Ching-Her Lee, Y. Yuan, and D. P. Nyquist, *Member, IEEE*

Abstract—A full-wave spectral-domain integral equation formulation is used to analyze coupled open-boundary microstrip transmission lines. A general rigorous formulation is specialized to the case of two identical uniform lines and a method of moments (MOM) solution is implemented. In contrast with earlier subdomain basis MOM solutions, entire-domain basis functions which incorporate appropriate edge conditions for transverse and longitudinal current components are utilized. This allows close-form evaluation of relevant spatial integrals and results in improved accuracy using far fewer terms. Numerical results in the form of propagation constants and current distributions are presented for the dominant and first two higher-order coupled modes, and compare favorably to results of other techniques.

I. INTRODUCTION

THE ANALYSIS of coupled microstrip transmission lines is a problem of both considerable practical interest, and of long history. Traditionally, various quasi-static methods (e.g., [1], [2]) have been used to compute the propagation characteristics of the coupled system. However, such methods are inherently inaccurate at higher frequencies, and are also found to be inadequate even at low frequencies for many useful combinations of substrate thickness and dielectric constant [3]. Additionally, in analysis of open systems potentially important surface-wave and radiation effects are neglected. In such cases a more accurate full-wave analysis must be utilized.

Recently a rigorous full-wave spectral-domain integral equation formulation has been advanced for analysis of generalized microwave integrated circuit configurations [4]. A subdomain basis MOM solution for coupled uniform microstrip transmission lines has been implemented, and yields accurate results in the form of current distributions and propagation constants for the dominant and several higher-order modes [5]. However, this method requires a large number of basis functions to achieve desired accuracy, yielding lengthy computation times.

In this work an entire-domain basis Galerkin's method

Manuscript received February 22, 1989; revised July 22, 1991. This work was supported by The Office of Naval Research under contracts N00012-86-K-0424 and N00014-86-K-0609.

J. S. Bagby is with the Department of Electrical Engineering, Florida Atlantic University, P. O. Box 3091, Boca Raton, FL 33431-0991.

C.-H. Lee is with the Department of Industrial Education, National Changhua University, Changhua, Taiwan 50058 R.O.C.

Y. Yuan and D. P. Nyquist are with the Department of Electrical Engineering, Michigan State University, East Lansing, MI 48824.

IEEE Log Number 9103902.

MOM solution of the integral equation formulation is implemented. The basis functions are carefully chosen to incorporate expected physical effects at the edges of the strips. Besides the advantage of allowing closed-form evaluation of relevant spatial integrals, it is found that excellent accuracy is obtained for as few as three basis functions for each current component of low-order modes, yielding compact approximate closed-form solutions for currents, as well as resulting in a substantial savings in computation time.

In Section II the mathematical formulation of the physical problem and the numerical solution technique utilized are introduced. The formulation is specialized to the case of natural modes of a pair of identical uniform coupled microstrip transmission lines. Numerical results in the form of propagation constants and strip current distributions (eigenvalues and eigenmodes) for the dominant and several higher-order eigenmodes of the coupled microstrip system are presented in Section III. Conclusions and areas for further investigation are discussed in Section IV.

II. FORMULATION

Consider the general open coupled microstrip geometry depicted in Fig. 1. A rigorous solution of Maxwell's equations results in a system of coupled integral equations satisfied by the unknown device surface currents [4]. For the axially-uniform systems as depicted in Fig. 2, an assumed propagation dependence of $\exp[j(\omega t - \xi z)]$ allows these equations to be simplified. For an arbitrary system of N uniform coupled microstrip transmission lines [5], the following axially-transformed coupled system of integral equations holds:

$$\hat{t}_j \cdot (\tilde{\nabla} \tilde{\nabla} \cdot + k_c^2) \sum_{i=1}^N \int_{\ell_i} \tilde{g}(\vec{\rho} \mid \vec{\rho}'; \xi) \cdot \vec{k}_i(\vec{\rho}') d\ell' = 0, \quad \vec{\rho} \in \ell_j, \quad j = 1, \dots, N \quad (1)$$

Here \vec{k}_i is the unknown axially-transformed eigenmode surface current on the i th strip, \tilde{g} is the transformed electric Hertzian potential Green's dyad of the microstrip background structure, ξ is the unknown eigenvalue (propagation constant) of the coupled mode, \hat{t}_j is a unit tangent to the j th strip, ℓ_i is the cross-sectional contour of the i th strip, and $\tilde{\nabla} = \nabla_i + j\xi z = (\partial/\partial x)\hat{x} + (\partial/\partial y)\hat{y} + j\xi z\hat{z}$ is the axially-transformed del-operator.

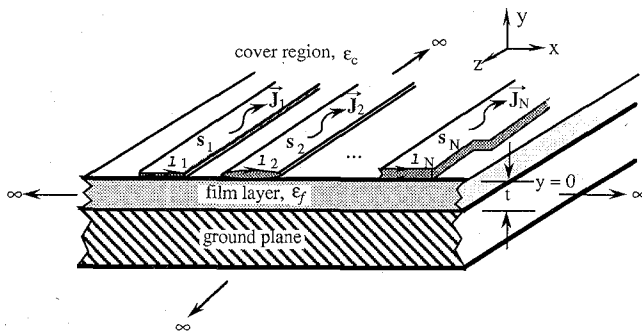


Fig. 1. Generalized system of N nonuniform coupled integrated microstrip transmission lines.

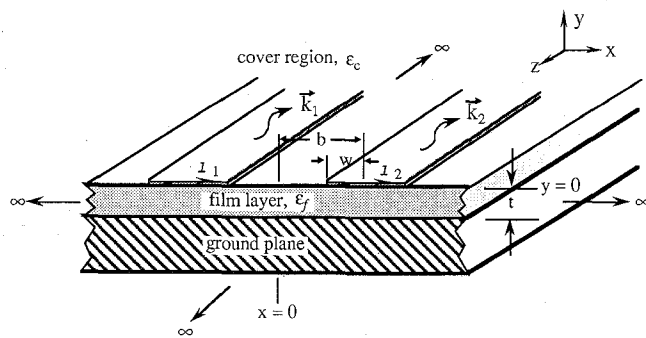


Fig. 2. Two identical axially-uniform thin coupled microstrip transmission lines.

The Hertzian potential Green's dyad decomposes into a principal and a reflected part, $\vec{g} = \vec{I}g^p + \vec{g}^r$, where g^p is the 2-dimensional unbounded-space Green's function in integral representation, and the reflected part has the dyadic form:

$$\vec{g}^r = \hat{x}g \pm \hat{x} + \hat{y} \left(\frac{\partial}{\partial x} g_c \hat{x} + g_n \hat{y} + j\zeta g_c \hat{z} \right) + \hat{z}g_t \hat{z}. \quad (2)$$

The scalar components of the reflected Green's dyad are given in terms of inverse-transform spectral integrals:

$$\left. \begin{aligned} g_t \\ g_n \\ g_c \end{aligned} \right\} = \int_{-\infty}^{\infty} \left\{ \begin{aligned} R_t(\lambda) \\ R_n(\lambda) \\ C(\lambda) \end{aligned} \right\} \frac{e^{j\zeta(x-x')} e^{-p_c(y+y')}}{4\pi p_c} d\xi. \quad (3)$$

The wavenumber parameters are defined as $\lambda^2 = \zeta^2 + \xi^2$, $p_c^2 = \lambda^2 - k_c^2$, $p_f^2 = \lambda^2 - k_f^2$, and the reflection and coupling coefficients are given by

$$\begin{aligned} R_t &= \frac{p_c - p_f \coth(p_f t)}{p_c + p_f \coth(p_f t)}; \quad R_n = \frac{K p_c - p_f \tanh(p_f t)}{K p_c + p_f \tanh(p_f t)} \\ C &= \frac{2(K-1)p_c}{[p_c + p_f \coth(p_f t)][K p_c + p_f \tanh(p_f t)]}; \\ K &= \frac{\epsilon_f}{\epsilon_c} \end{aligned} \quad (4)$$

A. Two Identical Microstrip Lines

Consider a simple coupled system consisting of a pair of identical open microstrip transmission lines. Assume that the lines are infinitely thin and are extended axially to infinity, as shown in Fig. 2, where b is half of the spacing between the centers of the two microstrip lines and w is half of the strip width. In this case (1) reduces to

$$\begin{aligned} \hat{t}_j \cdot \lim_{y \rightarrow 0} \sum_{i=1}^2 \int_{\ell_i} (k_c^2 + \tilde{\nabla} \tilde{\nabla} \cdot) \vec{g}(\vec{p} | x', y' = 0; \zeta) \\ \cdot \vec{k}_i(x', y' = 0; \zeta) dx' = 0; \quad j = 1, 2 \end{aligned} \quad (5)$$

where interchange of differentiation and integration is valid when $y \neq 0$. As $y \rightarrow 0$ the contour of spatial integration is a path along the x -axis, denoted ℓ_{x_i} . The tangential unit vector and the surface current decompose as $\hat{t} = \hat{x}t_x + \hat{z}t_z$; $\vec{k} = \hat{x}k_x + \hat{z}k_z$. To evaluate (5) we rewrite the integral representations of the scalar components g^p and $g_{t,n,c}$ as

$$\begin{aligned} g_{t,n,c}^p(\vec{r} | x'; \zeta) &= \int_{-\infty}^{\infty} i_{t,n,c}^p(\vec{r} | x'; \xi, \zeta) d\xi \\ i^p &= \frac{e^{j\zeta(x-x')} e^{-p_c|y|}}{4\pi p_c} \\ \left. \begin{aligned} i_t \\ i_n \\ i_c \end{aligned} \right\} &= \left\{ \begin{aligned} R_t \\ R_n \\ C \end{aligned} \right\} \frac{e^{j\zeta(x-x')} e^{-p_c y}}{4\pi p_c}. \end{aligned} \quad (6)$$

Substituting (6) into (5) in the limit $y \rightarrow 0$ yields two coupled integral equations by letting $\hat{t} = \hat{x}$ and $\hat{t} = \hat{z}$. They are

$$\begin{aligned} \hat{x} \cdot \sum_{i=1}^2 \int_{\ell_{x_i}} \int_{-\infty}^{\infty} \frac{e^{j\zeta(x-x')}}{4\pi p_c} [k_c^2(1 + R_i) k_x \\ - \xi(1 + R_i - p_c C)(\xi k_x + \xi k_z)] d\xi dx' = 0 \end{aligned} \quad (7a)$$

$$\begin{aligned} \hat{z} \cdot \sum_{i=1}^2 \int_{\ell_{x_i}} \int_{-\infty}^{\infty} \frac{e^{j\zeta(x-x')}}{4\pi p_c} [k_c^2(1 + R_i) k_z \\ - \xi(1 + R_i - p_c C)(\xi k_x + \xi k_z)] d\xi dx' = 0. \end{aligned} \quad (7b)$$

The final form of the equations for the coupled microstrip structure is obtained by resolving integration paths as $\ell_{x1} = [-b-w, -b+w]$ and $\ell_{x2} = [b-w, b+w]$:

$$\begin{aligned} \hat{x} \cdot \int_{-b-w}^{-b+w} \int_{-\infty}^{\infty} \frac{e^{j\zeta(x-x')}}{4\pi p_c} [k_c^2 R k_{x1} - \xi(R - C') \\ \cdot (\xi k_{x2} + \xi k_{z1})] d\xi dx' \\ + \int_{b-w}^{b+w} \int_{-\infty}^{\infty} \frac{e^{j\zeta(x-x')}}{4\pi p_c} [k_c^2 R k_{x2} - \xi(R - C') \\ \cdot (\xi k_{x2} + \xi k_{z2})] d\xi dx' = 0 \end{aligned} \quad (8a)$$

$$\hat{z}: \int_{-b-w}^{-b+w} \int_{-\infty}^{\infty} \frac{e^{j\xi(x-x')}}{4\pi p_c} [k_c^2 R k_{z1} - \zeta(R - C')] \\ \cdot (\xi k_{x1} + \zeta k_{z1}) d\xi dx' \\ + \int_{b-w}^{b+w} \int_{-\infty}^{\infty} \frac{e^{j\xi(x-x')}}{4\pi p_c} [k_c^2 R k_{z2} - \zeta(R - C')] \\ \cdot (\xi k_{x2} + \zeta k_{z2}) d\xi dx' = 0. \quad (8b)$$

Here k_{x1} , k_{z1} , and k_{x2} , k_{z2} are the transformed transverse and axial current components on strips 1 and 2, respectively, and

$$R = 1 + R_t = \frac{2p_c}{p_c + p_f \coth(p_f t)}$$

$$C' = p_c C = \frac{2(K-1)p_c^2}{[p_c + p_f \coth(p_f t)][Kp_c + p_f \tanh(p_f t)]} \quad (9)$$

Equation (8a) and (8b) are the appropriate coupled integral equations for natural modes of the uniform microstrip structure of Fig. 2. They have a nontrivial solution only when $\zeta = \zeta_m$ is an eigenvalue of the coupled system, where $m = 0, 1, \dots$ is the corresponding eigenmode number. They are further simplified by taking advantage of the symmetry in x inherent in the coupled structure. This allows the coupled equations can be written in terms of just one set of microstrip currents, where the other set is taken as the appropriate symmetric or antisymmetric extension. We now turn to a MOM solution of the coupled integral equations using entire-domain basis functions.

B. Entire-Domain Basis MOM Solution

The effectiveness of a MOM solution for (8) depends on a judicious choice of basis functions. These basis functions should incorporate as closely as possible the physical conditions of the actual axial and transverse currents on the microstrip. An overriding concern here is in the proper behavior of current components at the edges of the microstrip lines. In this work, instead of using subdomain basis functions which permit solutions satisfying the electromagnetic boundary conditions only at discrete points, we use entire-domain basis functions for expansion of the unknown surface currents and for testing the results (Galerkin's method). If the basis functions used closely resemble the unknown to be represented, the numerical solution will yield results of increased accuracy using far fewer terms.

It is a well known fact that the current distribution is singular at the edges of an isolated microstrip. According to Maxwell [6], the surface charge density distribution on an isolated strip (in the absence of a film layer) is $\sigma(x) = \sigma_0 / \pi \sqrt{1 - (x/w)^2}$, where σ_0 is the total charge on the strip and w is half-width of the strip. In the dynamic case, this distribution applies to the TEM solution for the longitudinal surface current as long as the ground-plane is

spaced far enough away from the strip [7]. For real hybrid-mode analysis, we can assume as a first step that the longitudinal current distribution of the fundamental mode follows the pattern of a pure TEM mode, and can be expressed approximately as $k_z(x') \cong v\sigma(x')$, where v is the phase velocity. The corresponding transverse current distribution can be obtained by use of the continuity equation $\partial k_x(x') / \partial x + j\zeta k_z(x') \cong -j\omega\sigma(x')$ [5]. For any microstrip eigenmode the longitudinal current is singular at the edges of the strip, while the transverse current is zero there. The transverse current is usually small compared to the longitudinal current (in the following analysis, it is at least one order of magnitude smaller) and its magnitude is proportional to the normalized strip width.

Based on the discussion above, it is found that Chebyshev polynomials multiplied by appropriate edge-factors are suitable expansion functions for eigenmodes of this structure. We choose Chebyshev polynomials of the second kind, $U_n(x)$, to expand the transverse eigenmode currents; the latter can accurately be represented by a linear combination of just few functions of this kind. Similarly, Chebyshev polynomials of the first kind, $T_n(x)$, are used for axial current expansion. Use of these weighted functions has the additional advantage of allowing relevant spatial integrals to be evaluated in closed form. Other examples of use of weighted Chebyshev polynomials as basis functions can be found (e.g., [8]). An instructive comparison of the convergence properties of weighted Chebyshev polynomials and regular trigonometric function is given in [9]. Based on this discussion, we expand the unknown currents as follows:

$$k_x(x') \cong \sqrt{1 - \left(\frac{x' - b}{w}\right)^2} \sum_{n=0}^{N-1} a_n U_n \left(\frac{x' - b}{w}\right)$$

$$k_z(x') \cong \frac{1}{\sqrt{1 - \left(\frac{x' - b}{w}\right)^2}} \sum_{n=0}^{N-1} b_n T_n \left(\frac{x' - b}{w}\right). \quad (10)$$

Here a_n and b_n are the usual known expansion coefficients representing the contribution of each order of Chebyshev polynomials $U_n(x)$ and $T_n(x)$ to the unknown surface currents, and the square-root factors in front of the summation terms give the anticipated edge behavior. To test the coupled equations we follow Galerkin's method and utilize the same functions for testing. Tabulated integrals in [10] and the Appendix are used for the calculations involved, yielding the following equations for symmetric eigenmodes of the coupled structure:

$$\hat{x}: \sum_{n=0}^{N-1} a_n (n+1) \int_{-\infty}^{\infty} \frac{e^{j\xi b}}{\xi^2 p_c} T_1 [k_c^2 R - \xi^2 (R - C')] \\ \cdot J_{m+1}(\xi w) J_{n+1}(\xi w) d\xi - \sum_{n=0}^{N-1} b_n w \xi \int_{-\infty}^{\infty} \frac{e^{j\xi b}}{p_c} \\ \cdot T_1 (R - C') J_{m+1}(\xi w) J_n(\xi w) d\xi = 0 \quad (11a)$$

$$\begin{aligned}
\hat{z}: & \sum_{n=0}^{N-1} a_n(n+1) \xi \int_{-\infty}^{\infty} \frac{e^{j\xi b}}{p_c} T_1(R - C') J_m(\xi w) \\
& \cdot J_{n+1}(\xi w) d\xi - \sum_{n=0}^{N-1} b_n w \int_{-\infty}^{\infty} \frac{e^{j\xi b}}{p_c} \\
& \cdot T_1[k_c^2 R - \xi^2(R - C')] J_m(\xi w) J_n(\xi w) d\xi = 0. \tag{11b}
\end{aligned}$$

Similarly, for antisymmetric modes we have

$$\begin{aligned}
\hat{x}: & \sum_{n=0}^{N-1} a_n(n+1) \int_{-\infty}^{\infty} \frac{je^{j\xi b}}{\xi^2 p_c} T_2[k_c^2 R - \xi^2(R - C')] \\
& \cdot J_{m+1}(\xi w) J_{n+1}(\xi w) d\xi - \sum_{n=0}^{N-1} b_n w \xi \int_{-\infty}^{\infty} \frac{je^{j\xi b}}{p_c} \\
& \cdot T_2(R - C') J_{m+1}(\xi w) J_n(\xi w) d\xi = 0 \tag{12a}
\end{aligned}$$

$$\begin{aligned}
\hat{z}: & \sum_{n=0}^{N-1} a_n(n+1) \xi \int_{-\infty}^{\infty} \frac{je^{j\xi b}}{p_c} T_2(R - C') J_m(\xi w) \\
& \cdot J_{n+1}(\xi w) d\xi - \sum_{n=0}^{N-1} b_n w \int_{-\infty}^{\infty} \frac{je^{j\xi b}}{p_c} \\
& \cdot T_2[k_c^2 R - \xi^2(R - C')] J_m(\xi w) J_n(\xi w) d\xi = 0. \tag{12b}
\end{aligned}$$

Here $T_1 = \cos(\xi b) \operatorname{Re}\{j^n\} - \sin(\xi b) \operatorname{Im}\{j^n\}$, $T_2 = \cos(\xi b) \operatorname{Im}\{j^n\} + \sin(\xi b) \operatorname{Re}\{j^n\}$. Integration limits on the spectral variable ξ can be further reduced by consideration of the parity of the integrands; the results have integration limits $[0, \infty)$. The final equations can be written in matrix form as

$$\begin{bmatrix} Z_{xx} & Z_{xz} \\ Z_{zx} & Z_{zz} \end{bmatrix} \begin{bmatrix} a_0 \\ \vdots \\ a_{N-1} \\ b_0 \\ \vdots \\ b_{N-1} \end{bmatrix} = 0. \tag{13}$$

Each element in the $(2N \times 2N)Z$ matrix is in terms of a spectral integral on ξ , and $a_0, \dots, a_{N-1}, b_0, \dots, b_{N-1}$ are the unknown coefficients for the expansion polynomials. To obtain a non-trivial solution the determinant of the coefficient matrix must vanish; since matrix elements depend on the unknown propagation constant ξ , we can iterate to find eigenvalues ξ_m for system eigenmodes. Numerical results of this technique are given in the next section.

III. NUMERICAL RESULTS

The method described above was implemented to calculate propagation constants (eigenvalues) and currents (eigenmodes) for the fundamental and higher order modes

TABLE I
EIGENVALUES

b/w	Mode	10 GHz EH ₀	20 GHz EH ₁	40 GHz EH ₂	
Isolated	1.10	3.00638	2.17164	2.23297	Symmetric modes
	1.25	2.98567	2.12381	2.21197	
	1.50	2.95200	2.09482	2.19654	
	2.89586	2.06867	2.17533		
Antisymmetric modes	1.50	2.83309	2.05419	2.15925	Antisymmetric modes
	1.25	2.78686	2.01026	2.11995	
	1.10	2.75250	1.94495	2.05663	

of the uniform coupled microstrip structure of Fig. 2. For convenience in comparison with other results [11], [12] the case $n_f = k_f/k_o = 3.13$, $n_c = 1.0$, $t = 0.635$ mm, $w = 1.5$ mm and a varying separation b is presented here.

A. Eigenvalues

Table I shows eigenvalues (normalized propagation constants) for the fundamental and first two higher coupled modes at operating frequencies near cutoff. Each coupled mode is seen to agree with the well known fact that $\xi_a < \xi_{iso} < \xi_s$, where ξ_a , ξ_{iso} , and ξ_s are eigenvalues corresponding to antisymmetric, isolated, and symmetric coupled modes, respectively. Also, the smaller the strip separation b/w , the larger (smaller) the eigenvalues for symmetric (antisymmetric) system modes, respectively. When the separation of the coupled strips is large enough (about $b/w \geq 4$), the eigenvalues converge to the corresponding isolated one; indeed, the symmetric and antisymmetric modes can be viewed as emerging from the corresponding isolated mode. Fig. 3 shows the dispersion curve for the coupled fundamental EH₀ mode. As strip separation decreases eigenvalues of the EH₀ symmetric and antisymmetric system modes are separate further; ultimately, when the strips contact on inside edges, the EH₀ symmetric mode goes to the EH₀ mode of an isolated strip with double width, and the EH₀ antisymmetric mode goes to the EH₁ mode of the same width-doubled strip, as expected. Eigenvalues for EH₀ and EH₁ modes over a wide range of frequency (up to 100 GHz) are calculated; the dispersion curves for several different separations are sketched in Figs. 4 and 5. The behavior of eigenvalues for this coupled structure are seen to be in good agreement with the results obtained by using the analysis in [1].

B. Eigenmode Currents

The axial and transverse current for each mode mentioned above are shown in Figs. 6–8. In numerically quantifying currents we found three Chebyshev polynomials sufficient to accurately represent the surface current of low-order modes on the isolated microstrip. For currents on each microstrip of the coupled system, we utilized the first five polynomials to achieve a more accurate result. It is seen in the figures that due to the repulsion of the charge, currents for symmetric modes have smaller magnitude near the inside edge than at the outside edge,

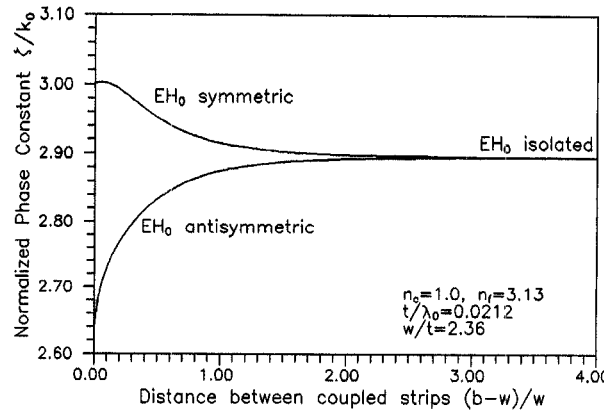


Fig. 3. Dependence of propagation constants (eigenvalues) ξ for dominant (EH_0) eigenmodes of two coupled microstrip lines upon line-to-line spacing; symmetric and antisymmetric coupled system modes are seen to emerge from the corresponding isolated line EH_0 mode.

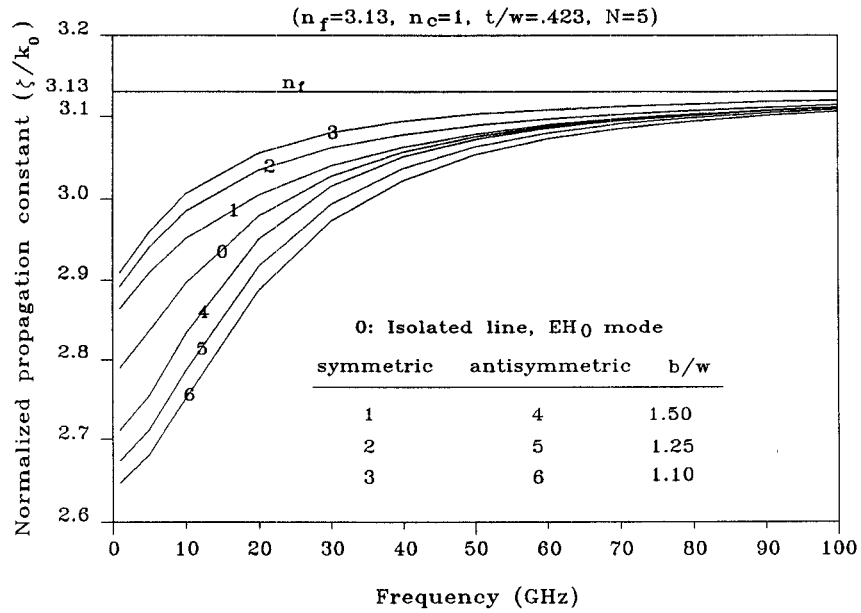


Fig. 4. Dispersion curves for isolated- and coupled-line fundamental modes (EH_0 eigenmodes).

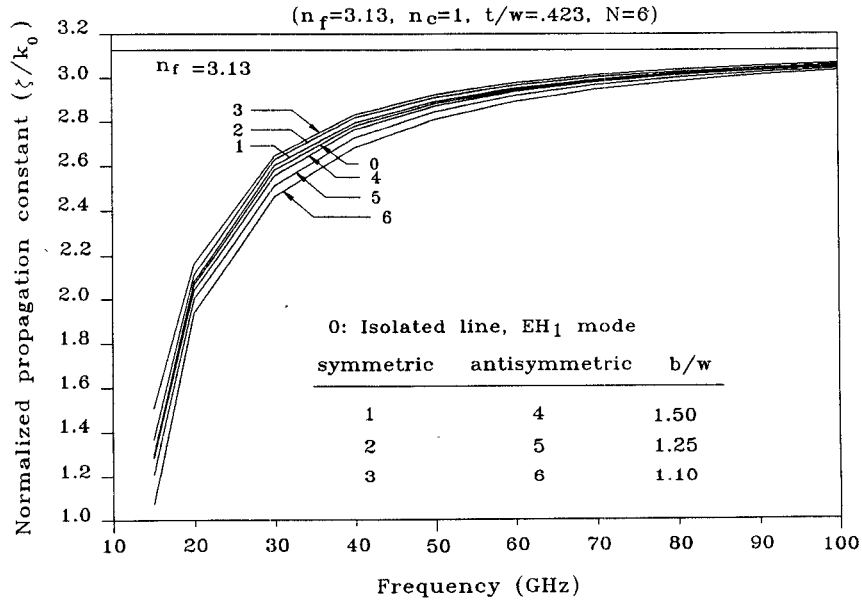


Fig. 5. Dispersion curves for isolated- and coupled-line first higher-order mode (EH_1 eigenmodes).

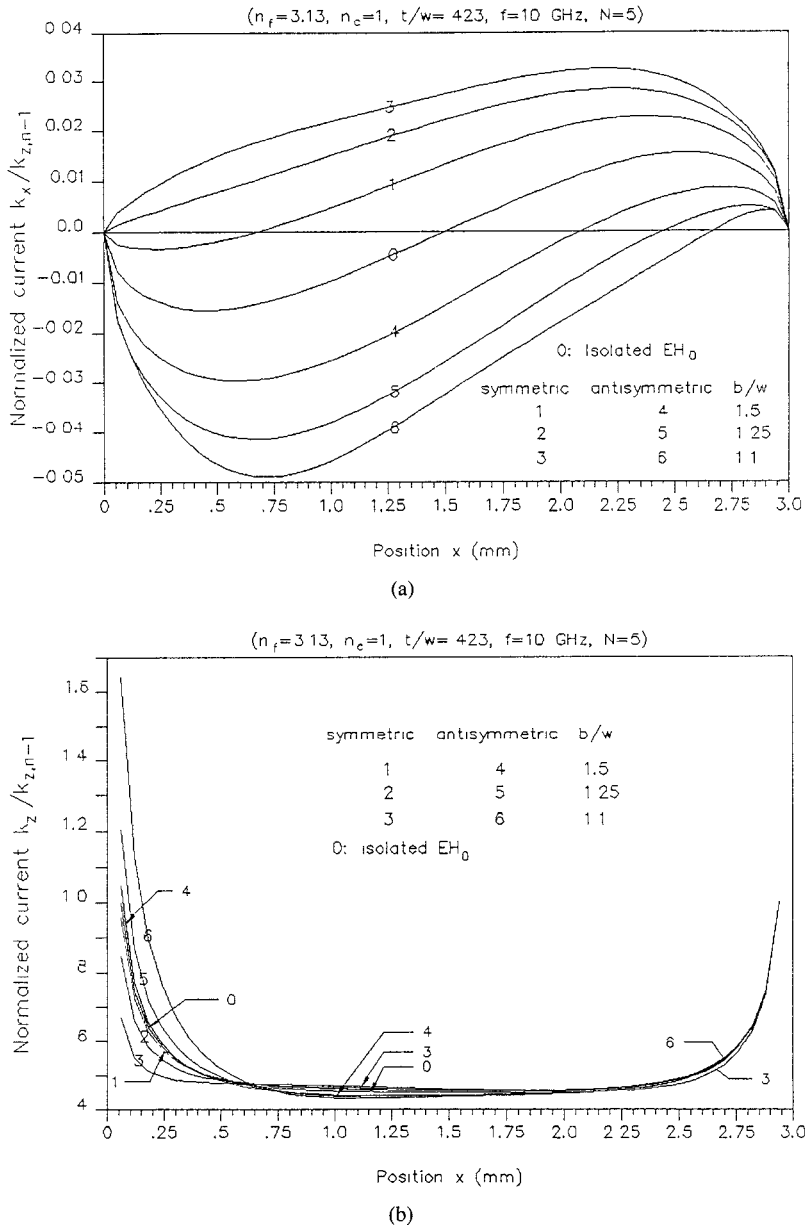


Fig. 6. Eigenmode currents for isolated and coupled dominant (EH_0) modes. (a) Transverse currents. (b) Axial currents.

a result intuitively expected. Similarly, antisymmetric modes have larger currents near the inside edge. In all cases, we can see that currents for isolated line lie between the two groups of currents of symmetric and antisymmetric system modes.

IV. CONCLUSION

A rigorous full-wave spectral-domain integral equation formulation has been presented for accurate analysis of coupled microstrip transmission lines. A method of moments solution utilizing entire-domain basis functions and Galerkin's method, incorporating appropriate edge conditions for transverse and longitudinal current components, permits closed-form evaluation of relevant spatial integrals. In contrast with earlier subdomain basis solutions, improved accuracy is obtained using far fewer

terms. Numerical results in the form of propagation constants and current distributions for the dominant and first two higher-order modes compare favorably to results of other techniques.

A more difficult problem which can be rigorously treated by the formulation presented here is the solution in the case of coupled microstrip transmission lines operating in lossy regimes, where excitation of surface waves and the radiation spectrum in the integrated circuit background structure could provide dominant coupling effects. This condition occurs when the propagation constant of the coupled system falls below the eigenvalue of a surface-wave mode supported by the integrated circuit background slab waveguide structure. In this case singularities in the spectral integrands move close to the real axis, and complex-plane evaluation techniques become

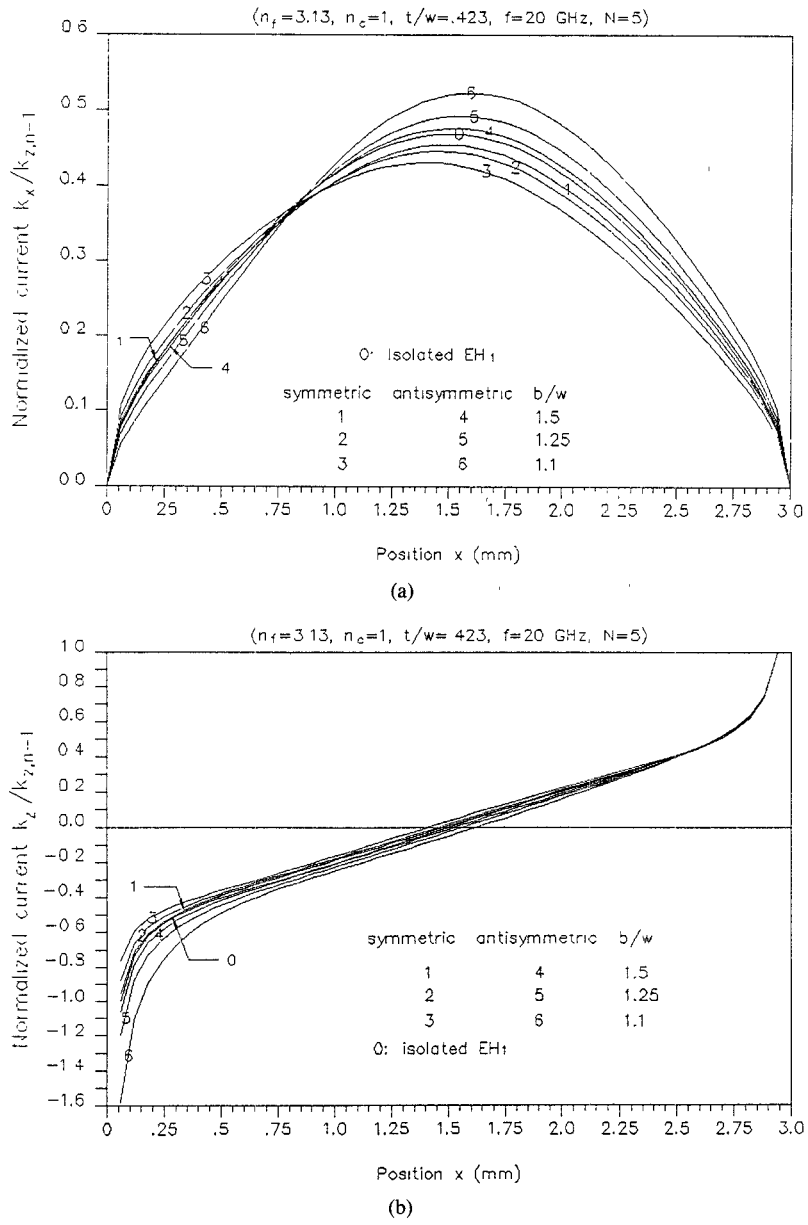


Fig. 7. Eigenmode currents for isolated and coupled first higher-order (EH₁) modes. (a) Transverse currents. (b) Axial currents.

necessary. Work along these lines is proceeding, and is expected to yield results in the near future [13]–[15].

APPENDIX

Other than the tabulated integral formulas in [10] we need to evaluate following integrals:

$$\begin{aligned}
 & \int_{-1}^1 \sqrt{1-x^2} \cos ax U_n(x) dx \\
 & \int_{-1}^1 \sqrt{1-x^2} \sin ax U_n(x) dx \\
 & \int_{-1}^1 \cos ax T_n(x) \frac{dx}{\sqrt{1-x^2}} \\
 & \int_{-1}^1 \sin ax T_n(x) \frac{dx}{\sqrt{1-x^2}}. \quad (A1)
 \end{aligned}$$

$$\begin{aligned}
 & \int_{-1}^1 (1-x^2)^{v-1/2} e^{i a x} C_n^v(x) dx \\
 & = \frac{\pi 2^{1-v} i^n \Gamma(2v+n)}{n! \Gamma(v)} a^{-v} J_{v+n}(a). \quad (A2)
 \end{aligned}$$

Using the fact $U_n(x) = C_n^{(1)}(x)$, which relates Chebyshev to Gegenbauer polynomials, the above formula yields the results:

$$\begin{aligned}
 & \int_{-1}^1 \sqrt{1-x^2} \cos ax U_n(x) dx \\
 & = \frac{\pi(n+1)}{a} J_{n+1}(a) \operatorname{Re} \{i^n\}
 \end{aligned}$$

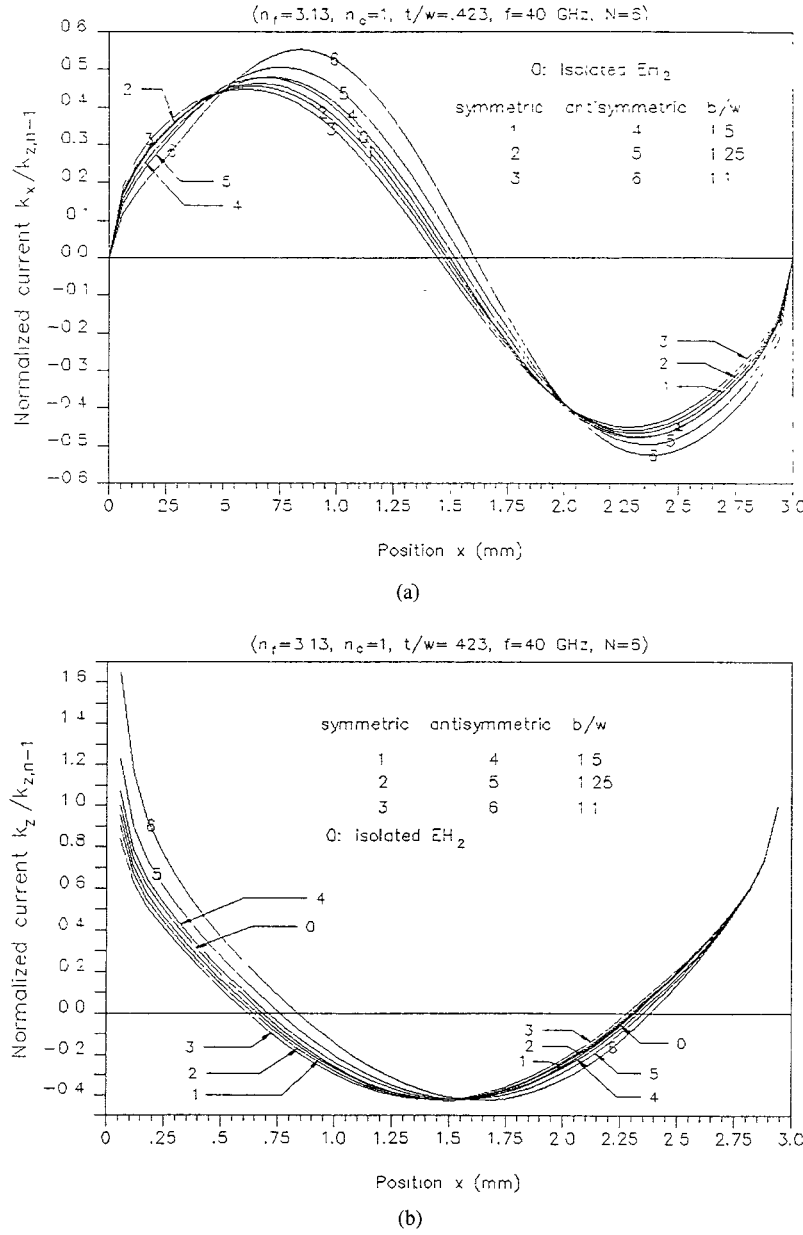


Fig. 8. Eigenmode currents for isolated and coupled second higher-order (EH₂) modes. (a) Transverse currents. (b) Axial currents.

$$\begin{aligned} & \int_{-1}^1 \sqrt{1-x^2} \sin ax U_n(x) dx \\ &= \frac{\pi(n+1)}{a} J_{n+1}(a) \operatorname{Im} \{i^n\}. \end{aligned} \quad (\text{A3})$$

A similar procedure can be used for evaluating the remaining integrals; refer to equation (7-355), p. 836 of [10]:

$$\begin{aligned} & \int_0^1 T_{2n+1}(x) \sin ax \frac{1}{\sqrt{1-x^2}} dx = (-1)^n \frac{\pi}{2} J_{2n+1}(a) \\ & \int_0^1 T_{2n} \cos ax \frac{dx}{\sqrt{1-x^2}} = (-1)^n \frac{\pi}{2} J_{2n}(a). \end{aligned} \quad (\text{A4})$$

From this we obtain the results:

$$\begin{aligned} & \int_{-1}^1 \cos ax T_n(x) \frac{dx}{\sqrt{1-x^2}} \\ &= \begin{cases} 0, & \text{for odd } n, \\ (-1)^{n/2} \pi J_n(a), & \text{for even } n. \end{cases} \\ & \int_{-1}^1 \sin ax T_n(x) \frac{dx}{\sqrt{1-x^2}} \\ &= \begin{cases} (-1)^{(n-1)/2} \pi J_n(a), & \text{for odd } n, \\ 0, & \text{for even } n. \end{cases} \end{aligned} \quad (\text{A5})$$

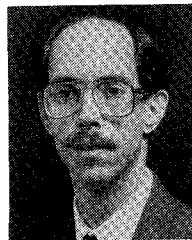
Further algebra provides the following integral formulas for use:

$$\begin{aligned} \int_{-1}^1 \cos axT_n(x) \frac{dx}{\sqrt{1-x^2}} &= \operatorname{Re} \{ i^n \pi J_n(a) \} \\ &= \pi J_n(a) \operatorname{Re} \{ i^n \} \\ \int_{-1}^1 \sin axT_n(x) \frac{dx}{\sqrt{1-x^2}} &= \operatorname{Im} \{ i^n \pi J_n(a) \} \\ &= \pi J_n(a) \operatorname{Im} \{ i^n \} \quad (A6) \end{aligned}$$

REFERENCES

- [1] K. C. Gupta, R. Garg, and I. J. Bahl, *Microstrip Lines and Slotlines*. Norwood, MA: Artech House, 1979, p. 303.
- [2] E. G. Farr, C. H. Chan, and R. Mittra, "A frequency-dependent coupled-mode analysis of multiconductor microstrip lines with application to VLSI interconnection problems," *IEEE Trans. Microwave Theory Tech.*, vol. MTT-34, no. 2, pp. 307-310, Feb. 1986.
- [3] J. R. Mosing and T. K. Sarkar, "Comparison of quasi-static and exact electromagnetic fields from a horizontal electric dipole above a lossy dielectric backed by an imperfect ground plane," *IEEE Trans. Microwave Theory Tech.*, vol. MTT-34, no. 4, pp. 379-387, Apr. 1986.
- [4] J. S. Bagby and D. P. Nyquist, "Dyadic Green's function for integrated electronic and optical circuits," *IEEE Trans. Microwave Theory Tech.*, vol. MTT-35, no. 2, pp. 206-210, Feb. 1987.
- [5] C.-H. Lee and J. S. Bagby, "Analysis of coupled microstrip transmission lines with EFIE method," in *Proc. 1988 Int. Radio Science (URSI) Meeting*, Syracuse, NY, June 1988, p. 318.
- [6] J. C. Maxwell, *A Treatise on Electricity and Magnetism*, 3rd ed., vol. 1, New York: Dover, 1954, pp. 296-297.
- [7] E. J. Denlinger, "A frequency dependent solution for microstrip transmission lines," *IEEE Trans. Microwave Theory Tech.*, vol. MTT-19, no. 1, pp. 30-39, Jan. 1971.
- [8] E.-B. El-Sharawy and R. W. Jackson, "Coplanar waveguide and slot line on magnetic substrates: analysis and experiment," *IEEE Trans. Microwave Theory Tech.*, vol. 31, no. 6, pp. 1071-1079, June 1988.
- [9] A. Frenkel, "On entire-domain basis functions with square-root edge singularity," *IEEE Trans. Antennas Propagat.*, vol. AP, no. 9, pp. 1211-1214, Sept. 1989.
- [10] I. S. Gardshteyn and I. M. Ryzhik, *Table of Integrals, Series, and Products*. New York: Academic Press, 1980, p. 836.
- [11] H. Ermert, "Guiding and radiation characteristics of planar waveguides," *IEE Microwave, Optics and Acoustics*, vol. 3, pp. 59-62, Mar. 1979.
- [12] A. A. Oliner, "Leakage from higher modes on microstrip line with application to antennas," *Radio Sci.*, vol. 22, no. 6, pp. 907-912, Nov. 1987.
- [13] K. A. Michalski and D. Zheng, "Rigorous analysis of open microstrip lines of arbitrary cross-section in bound and leaky regimes," *IEEE Trans. Microwave Theory Tech.*, to be published.

- [14] J. S. Bagby, C.-H. Lee, D. P. Nyquist and Y. Yuan, "Propagation region on integrated microstrip lines," *IEEE Trans. Microwave Theory Tech.*, to be published.
- [15] C.-H. Lee, *Integral Equation Analysis of Microstrip Transmission Lines*, Ph.D. dissertation, the University of Texas at Arlington, Dec. 1989.



Jonathan S. Bagby was born in Denville, NJ, in 1957. He received the B.S. degree in 1980 from Michigan State University, the M.S. degree in 1981 from Ohio State University, and the Ph.D. degree from Michigan State University in 1984, all in electrical engineering.

From 1984 to 1991 he was an Assistant Professor of Electrical Engineering at the University of Texas at Arlington, and since 1991 has been an Associate Professor of Electrical Engineering at Florida Atlantic University. His research interests

include microwave integrated circuits, integrated optical circuits, radar/radome interactions, electromagnetic radiation and scattering, and guided wave optics.

Dr. Bagby is a member of Eta Kappa Nu, Tau Beta Pi, Sigma Xi, and Phi Kappa Phi. He was the recipient of the 1983 MSU Excellence in Teaching Citation, and was named the UTA College of Engineering Outstanding Young Faculty Member in 1989.



Ching-Her Lee was born in Pingtung Taiwan, in 1954. He received the B.S. and M.S. degree in electronic and automatic control engineering from Feng-Chia University, Taichung, Taiwan, in 1977 and 1981, respectively, and the Ph.D. degree in electrical engineering from The University of Texas at Arlington in 1989.

From 1981 to 1985, he was on the faculty of Chin-Yih Institute of Technology, Taichung, Taiwan, where he was the head of Electronic Engineering Department. While there, his specialty was high frequency circuit designs. He is currently an Associate Professor at National Changhua University of Education, Changhua, Taiwan. His research interests include microstrip devices, dielectric optical waveguides, and numerical methods and electromagnetics.

Dr. Lee is a member of the Tau Beta Pi and The Chinese Institute of Engineers. He was a Recipient of the Cash Award of Youth's Development and Invention and Award of Technical Invention of 1982, which is sponsored by the Ministry of Education, Republic of China (at Taiwan).

Y. Yuan, photograph and biography not available at the time of publication.

D. P. Nyquist (S'63-M'67), photograph and biography not available at the time of publication.